Journal of Applied Mechanics and Technical Physics, Vol. 37, No. 4, 1996

NUMERICAL SIMULATION OF SUPERSONIC SEPARATED TURBULENT FLOWS

A. V. Borisov and N. N. Fedorova

UDC 518.517.4

The wide occurrence of separated flows in nature and practice stimulates interest in their experimental and numerical investigation. The main difficulties in mathematical modeling of such flows are due to the fact that the separation of a boundary layer is a three-dimensional nonstationary physical process that must be described by full Navier–Stokes equations. In studies of flows at high Reynolds numbers, turbulence modeling and associated closure of initial equations are very important. In supersonic separated flows, the occurrence of separation is most often caused by the shock-wave–boundary-layer interaction and accompanied by the occurrence of additional disturbances during the process of viscous-nonviscous interaction. In these case, it is important to describe adequately gas-dynamic flow patterns with a high resolution of discontinuities. The development of modern numerical methods for solving Euler equations allows one to predict the wave structure of supersonic flows rather closely. Hopefully, the development of similar methods for Navier–Stokes equations will enable one to describe more accurately the gas-dynamic features under conditions of strong viscous-nonviscous interaction and to model separated flows more adequately.

In previous investigations concerned with numerical modeling of turbulent separated flows either of compressible or incompressible fluids, most attention has been given to the analysis of potentials of the turbulence models used [1–3]. Although it is generally agreed that development of a universal turbulence model is not feasible, attempts to improve calculations of turbulent separations, primarily on the basis of a more exact description of pulsation and average features within more and more complicated semiempirical models, are continuing. Without denying the importance of a turbulence model, particularly for correct computation of the surface-friction and heat-transfer distributions in the interaction zones, we seek to study how the quality of numerical algorithms influences the accuracy of prediction of the gas-dynamic structure and scales of separated flows.

Two-dimensional supersonic boundary flows have been studied numerically by integrating the Favre-averaged Navier–Stokes equations [4]; the two-parameter $k - \omega$ turbulence model of [5] was used for closure of the equations. The calculations were performed by an implicit finite-difference scheme of the type of a universal algorithm [6] using splitting by physical processes and spatial variables [7]. Also, special higher-order approximations for nonviscous fluids and TVD ideology [8, 9] were used which demonstrated the high degree of resolution of gas-dynamic flow structure for Euler equations. The equations used, the turbulence model, and the finite-difference scheme are described in detail in [10].

Supersonic turbulent flows in the vicinity of compression and expansion angles, which were studied experimentally in [11–14], were calculated. The complete tabulated data of these experiments are given in [15]. The chosen configurations were two-dimensional oblique and right-angled steps which were placed on a plate and had $h = 15$ mm and face angles $\beta = 8$, 25, 45, and 90°. The flow structure in the vicinity of such configurations is characterized by the sequential interaction of the boundary layer with a shock wave and a fan of rarefaction waves, and depends greatly on the angle β and the Mach number of the incoming flow M_e. An increase in the angle β leads to an increase in the shock-wave intensity, which allows one to observe how the "flow picture" changes from a continuous situation to the formation of a large-scale separation zone.

Institute of Theoretical and Applied Mechanics, Russian Academy of Sciences, Novosibirsk 630090.
Translated from Prikladnaya Mekhanika i Tekhnicheskaya Fizika, Vol. 37, No. 4, pp. 89–97, July–August, 1996. Original article submitted May 16, 1995.

0021-8944/96/3704-0533 $15.00

TABLE 1

β, deg	M_e	$Re_1 \cdot 10^{-6}$, m^{-1}	P_0, kPa	T_0, K	δ	δ^*	δ^{**}	$C_f \cdot 10^{-3}$
					mm			
8	2.8	33.1	416.1	292	3.33	1.07	0.23	1.59
25	2.88	32.4	414.14	294	4.1	1.43	0.3	1.47
45	2.8	34.8	414.14	282	5.72	1.92	0.43	1.5
90	2.94	36.3	420.71	277	3.33	1.07	0.23	1.59

Use of flows with different sequences of interaction of boundary layers with shock and rarefaction waves as tests (see, for example, [16, 17]) makes it possible to evaluate the capability of numerical algorithms to reflect the gas-dynamic features due to viscous-nonviscous interaction. Solution of this problem also allows one to investigate the properties of turbulence models (used to close the general equations) for various types of disturbances.

Graur et al. [18, 19] have investigated the applicability of "kinetically consistent" finite-difference schemes for predicting turbulent separated flows using as an example flow past a right-angled step ($\beta = 90°$) studied experimentally in [11, 12]. Good agreement with the experimental data on the surface-pressure distribution for various Mach numbers of incoming flow was obtained. It is hardly probable, however, that the method used in the above-mentioned papers would be effective for predicting the friction and heat transfer due to viscous effects.

Hortsman and Zheltovodov [17] reported good agreement between the calculated and experimental surface friction and pressure distributions, and also between the distributions of velocity fields, density, Mach numbers, and integrated characteristics of the boundary layer. The computations were performed on a fine grid, using two turbulence models for oblique forward-facing steps with face angles up to $\beta = 45°$ and for backward-facing steps with $\beta = 8$ and 25°. It should be noted that within the developed numerical method the efforts to achieve higher values of face angles were not successful. The data in [20] show considerable improvement in numerical results using a more detailed grid.

Borisov et al. [21–23] reported the results of studies of flows in the vicinity of the above-mentioned configurations using first- and second-order approximation schemes for various turbulence models. For small angles β, correct and qualitative flow "pattern" and fair agreement with experiment for the distributions of the friction coefficient and surface pressure were obtained. At the same time, with an increase in β, the difference between experimental and calculated data becomes more considerable. The present paper is a continuation of the previous studies aimed at improving the quality of computation methods to achieve agreement between calculation and experiment for all flow parameters over a wide range of the angles β.

Let us consider some experimental conditions and the details of the calculations performed. A developed turbulence boundary layer formed at a considerable distance from the interaction zone in front of the obstacles on the plate surface. Table 1 lists the main incoming-flow and boundary-layer parameters (the Mach number above the plate M_e, the single Reynolds number Re_1, the pressure P_0, the stagnation temperature T_0, the thickness of the boundary layer δ, the displacement thickness δ^*, the momentum loss δ^{**}, and the surface friction coefficient C_f) that correspond to the experimental conditions of [15] for flows in the vicinity of steps with different angles β. The boundary conditions at the inlet section were obtained by solution of the problem of a boundary layer over a plate and by choice of the section x at which the calculated displacement thickness coincided with that determined experimentally (the difference between the calculated and experimental data did not exceed 1% for the parameters above the boundary layer and 5% for δ and δ^{**}). Correct assignment of the coefficient C_f in front of the interaction zone is very important, because precisely this coefficient determines the position of a separation point. With the above choice of the initial section by the displacement thickness the calculated and experimental values of C_f differed by 5–6 % (with experimental determination accuracy $C_f \approx$ 10–15 %), which guaranteed agreement between the calculated profile in front of the interaction zone and the experimental conditions.

The calculation domain was limited by the surface of the body and a number of sections chosen at a

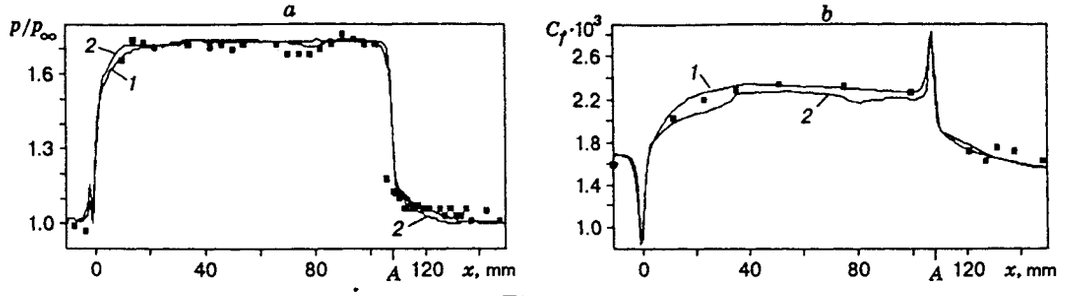

Fig. 1

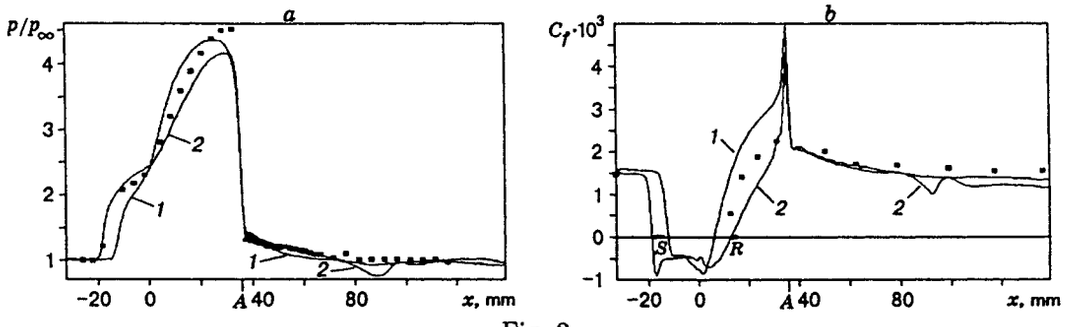

Fig. 2

sufficient distance from the interaction zone. The grid contained 100 to 250 points in the x direction and 90 to 150 points in the y direction and became finer exponentially toward the surface of the body. The fineness parameter was chosen so that the values of the law-of-the-wall variable y^+ at the grid points nearest to the surface of the body satisfied the condition $y^+ \leqslant 2$. The calculations were performed up to the wall on which conditions of attachment and nonexistence of thermal flow were assigned.

Figures 1–4 gives the surface-pressure (a) and friction (b) distributions for $\beta = 8$, 25, 45, and 90°, respectively, as a function of x, i.e., the distance measured from the vertex of the compression angle along the contour of the obstacle. Point A on the x axis is the coordinate of the vertex of the expansion angle. The symbols refer to the experimental data of [15] and curves 1 and 2 to the calculation results with first- and third-order approximations.

Figure 1 shows that the schemes of first and of higher-order approximations give practically similar results for weak interactions ($\beta = 8°$). As the angle β increases (Figs. 2–4), the difference between the calculated data increases. Calculations using the first-order scheme predict incorrectly the location of the region of pressure rise and separation and also the pressure level ("plateau") in the separation zone. Comparison of the calculated data obtained using the third-order approximation scheme with the experimental data indicates an improvement in the quality of prediction for the wave structure of the flow. The fact that the calculated pressures near the vortex of the expansion corner (point A, Figs. 2a and 3a) are lower than those obtained experimentally can be explained by decentering of the fan of Prandtl–Mayer waves which will be clear below from analysis of the gas-dynamic flow diagrams.

The graphs of the behavior of the surface-friction coefficient for various angles β (Figs. 2b-4b) show that the behavior of C_f obtained in calculations using the higher-order approximation scheme also agrees with the experimental data better than that determined by the first-order scheme. Note that the order of approximation has a significant effect on the location of separation and reattachment points correspond to $C_f = 0$. Points S and R in Figs. 2b–4b indicate positions of the separation and reattachment points determined in the experiment by oil-black visualization and also by velocity-profile measurements. Various methods gave somewhat different positions of these points. The spread of the experimental data is shown by the rectangles on the x axis. Figures 2b–4b give a comparison of the experimental and calculated lengths of separation zones

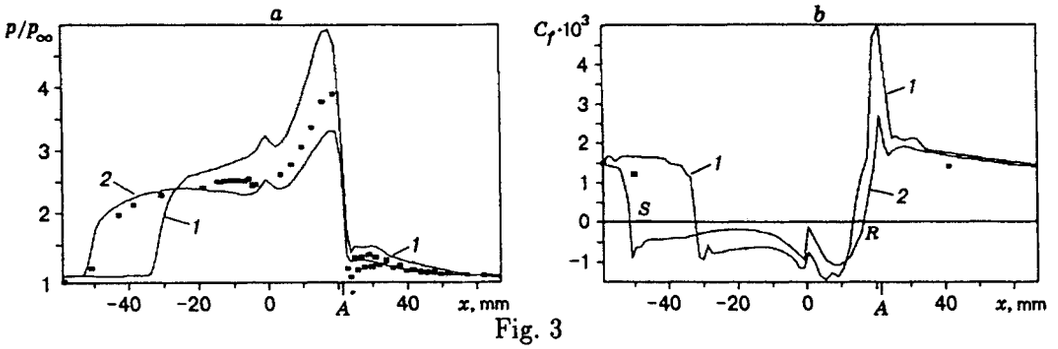

Fig. 3

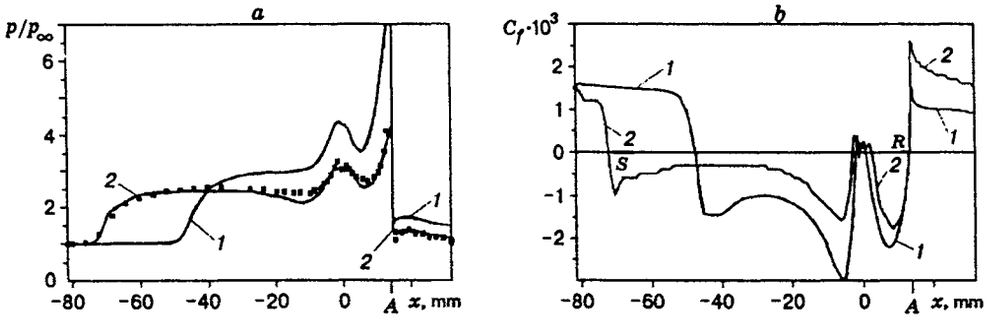

Fig. 4

between the separation and reattachment points. The coordinates of points S and R for the calculations with first-order (calculation 1) and third-order approximations (calculation 2), and also the experimental data of [15] are given in Table 2. It is obvious that higher-order approximation schemes allow one to predict rather exactly the scales of separated flows.

For turbulence modeling in a boundary layer, it is important to compare the calculated and experimental values of C_f within the separation zone. In [15], there is no information on the friction distribution in the reverse-flow zone because of limitation of the method used. The developed optical methods of friction measurements [24, 25] allow one to determine C_f over the entire region including separation zones. The comparison for a step with $\beta = 45°$ and $h = 5$ mm in [25] shows good agreement between the results of calculations using the approach described and the experimental data for the recirculation flow region.

Figure 5 gives the flow structure for $\beta = 8°$, which is plotted according to the experimental data (a), and the contours of the dimensionless total pressure $\tilde{P}_0 = P_0/\rho_\infty U_\infty^2$ obtained in calculations using the first-order (b) and third-order (c) approximation schemes. Curve 1 corresponds to a shock wave, 2 to a rarefaction-wave fan, and 3 to a boundary layer which is continuous for this angle. The number of contours is 30. The levels were chosen equidistantly between the minimum ($\tilde{P}_0 = 0$) and the maximum ($\tilde{P}_0 = 0.85$) pressure values. The positions of the sections for which the measurements were performed are denoted by circles in Fig. 5a. Analysis of the calculated data show that, although both schemes give correct predictions of wave intensity and position, the first-order scheme (Fig. 5b) "smears" substantially the shock wave and the rarefaction fan. In calculations using the third-order scheme (Fig. 5c), we assigned the maximum possible value of the scheme parameter that determines the degree of localization of wave fronts on the grid [26]. This made it to possible to determine the flow structure with sufficient accuracy, but, at the same time, gave rise to "noise" in the vicinity of the shock wave. The possible causes of the "noise" in numerical solution in the vicinity of stationary shock waves are investigated in [27].

The experimental flow pattern for $\beta = 25°$ is presented in Fig. 6a. Figures 6b and 6c give the calculated contours of the dimensionless static pressure $\tilde{p} = p/\rho_\infty U_\infty^2$ for first- and third-order approximations, respectively. The number of contours is 30, $\tilde{p}_{\min} = 0.06$ and $\tilde{p}_{\max} = 0.42$. The shock wave 1 caused by the

TABLE 2

Results of	β, deg					
	25		45		90	
	x_S	x_R	x_S	x_R	x_S	x_R
	mm					
Experiment [15]	−(15–18)	12–15	−(45–49)	15–16	−(65–70)	14
Calculation 1	−13	6	−31	14	−48	14
Calculation 2	−20	12	−51	18	−72	14

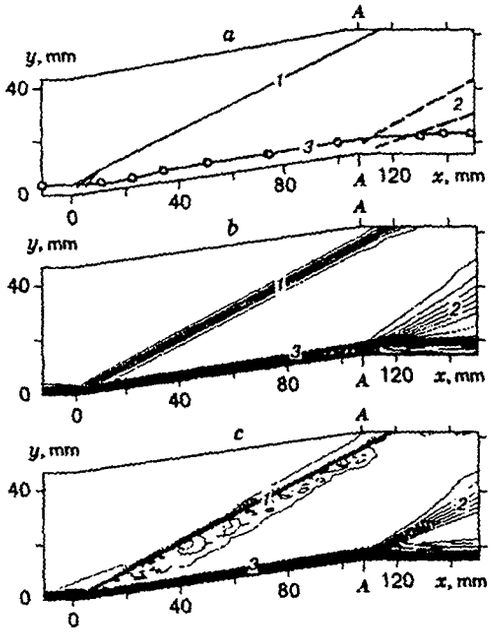

Fig. 5

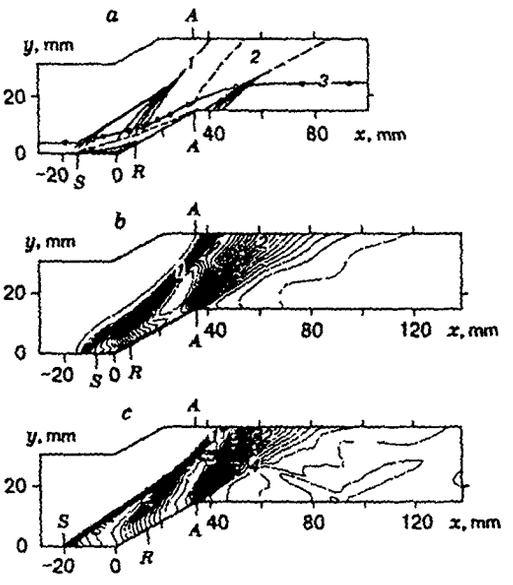

Fig. 6

existence of a compression angle is intense enough to separate the boundary layer. The boundaries of the separation zone determined by velocity profiles are shown by points S and R in Fig. 6a. An increase in the order makes it possible to find more exactly the size of the separation zone. A more exact location of the compression waves formed in the vicinities of separation and reattachment points allows the experimentally observed λ-configuration (Fig. 6c) to be obtained by calculations. The computations also show that a rarefaction fan 4, which cannot be clearly seen in experiments, emerges from the triple point. The fan causes the occurrence of a local zone with lower friction coefficient and pressure on the upper side of the step (Fig. 2, curves 2). This was not pronounced in experiments. The contact discontinuity was very weak and was determined only by the entropy function. It is important to note that such a flow structure is consistent and is supported by experiments (see [28], where the interaction of shock waves of various intensities was studied). In the calculation with a first-order approximation (Fig. 6b), the shock waves nearly merged into one wave because of the strong smearing and the λ-configuration was not observed.

Figure 7 presents the gas-dynamic flow structure determined experimentally (a) and that obtained in the calculations using the higher-order scheme (b) for $\beta = 45°$. Here curves 1 is a shock wave, curves 2 is a rarefaction fan, which is spreading from the step top (the dashed curves show extreme characteristics), curves 3 is the edge of the boundary layer, and curves 4 is a rarefaction fan; curves 5 correspond to M = 1, curves 6 to zero velocity, curves 7 to the maximum reverse velocity, and curves 8 to a dividing streamline. The point S in Fig. 7a corresponds to the position of a separation point determined from velocity profiles, and point R

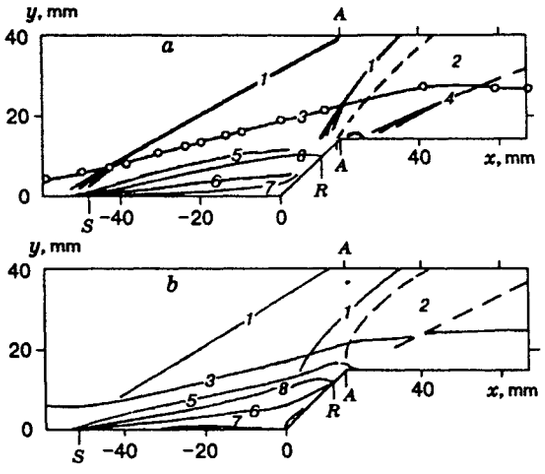

Fig. 7

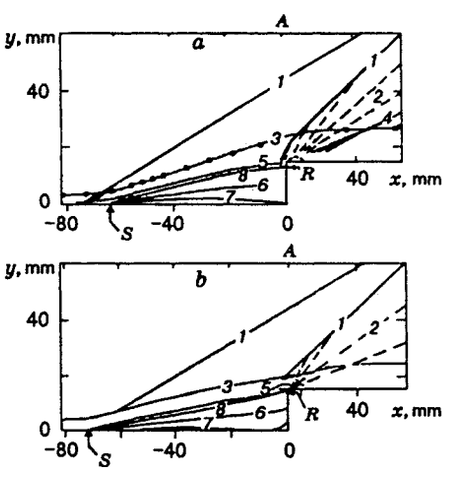

Fig. 8

corresponds to the position of a reattachment point determined using oil-black visualization. The calculation guarantees good agreement with the experiment for the wave structure, position of the characteristic flow lines, and also for the size of the separation zone (see Table 2).

Experimental (a) and calculated (b) flow diagrams past the first step $\beta = 90°$ are given in Fig. 8 (notation is the same as in Fig. 7). Comparison of the flow diagrams shows fairly good agreement of the wave structures of flow in the separation zone. The shock wave formed immediately in front of the butt-end decays rapidly in the calculations because of the interaction with the expansion wave. The compression waves denoted by Fig. 4 are also weak and are not observed in the calculations.

Thus, the calculations using the high-resolution scheme demonstrated good quality of prediction of the wave structure of flows formed under conditions of strong viscous-nonviscous interaction and separation of the turbulent boundary layer. Previous investigations using a different spatial approximation of initial equations did not give such good agreement between calculated and experimental data. The order of spatial approximation has the strongest effect on the accuracy of separated-flow calculations.

We are grateful to A. A. Zheltovodov, who initiated the present study, for providing the experimental data base, for fruitful discussion of the results, and for important corrections to the text; to S. I. Shpak who kindly supplied us with a program for graphical processing of calculated and experimental results; to Prof. D. Knight (Rutgers University, USA) for continuous attention to our work; and to Dr. M. Barrett (United Technologics Center for Integrated Technologies, USA) for financial support.

This work was supported by the Siberian Division of the Russian Academy of Sciences (within the framework of the competition of international projects for 1995) and by the Scientific Research Center of the Corporation for Integrated Technologies.

REFERENCES

1. J. S. Marvin, "Modeling of turbulent separated flows for aerodynamic applications," in: *Recent Advances in Aerodynamics*: Proc. of an Int. Symp. Held at Stanford University, Krothapalli and C. A. Smith (eds.), Aug. 22–26, 1982, Springer-Verlag, Berlin (1983).
2. J. S. Marvin and T. J. Coackley, "Turbulence modeling for hypersonic flows," NASA Tech. Memorandum 101079 (1989).
3. W. Rodi, "Recent developments in turbulence modeling," in: Proc. of 93 Workshop on Mathematical Modeling of Turbulent Flows, August, Japan (1993).
4. D. C. Wilcox, *Turbulence Modeling for CFD*, DCV Industries Inc., California (1993).

5. D. C. Wilcox, "Reassessment of the scale determining equation for advanced turbulence models," *AIAA J.*, **26**, No. 11, 1299–1310 (1988).
6. N. N. Yanenko, *Method of Fractional Steps in Solution of Multidimensional Problems of Mathematical Physics* [in Russian], Nauka, Novosibirsk (1967).
7. V. M. Kovenya and N. N. Yanenko, *A Splitting Method in Gas-Dynamic Problems* [in Russian], Nauka, Novosibirsk (1981).
8. Bram van Leer, "Towards the ultimate conservative difference scheme V: A second-order sequel to Godunov's method," *J. Comput. Phys.*, **32**, No. 1, 101–136 (1979).
9. A. Harten, "High resolution schemes for hyperbolic conservation laws," *J. Comput. Phys.*, **49**, No. 2, 357–393 (1979).
10. A. V. Borisov and N. N. Fedorova, "Calculation of turbulent separated flows using the method of higher-order approximations," *Teplofiz. Aeromekh.*, **2**, No. 3, 253–269 (1995).
11. A. A. Zheltovodov, "Analysis of the properties of two-dimensional separated flows at supersonic speeds," in: *Investigations of Boundary Flows of Viscous Gas*, Inst. Theor. and Appl. Mech., Sib. Div., Russian Acad. of Sciences, Novosibirsk (1979), pp. 59–94.
12. A. A. Zheltovodov and A. A. Pavlov, "Investigation of flow in a supersonic separation zone in front of a step," Preprint No. 1, Inst. Theor. and Appl. Mech., Sib. Div., Acad. of Sci. of the USSR, Novosibirsk (1979).
13. A. A. Zheltovodov, /'E. Kh. Shilein, and V. N. Yakovlev, "Development of a turbulent boundary layer under mixed interaction with shock and expansion waves," Preprint No. 28-83, Inst. Theor. and Appl. Mech., Sib. Div., Acad. of Sci. of the USSR, Novosibirsk (1983).
14. A. A. Zheltovodov and V. N. Yakovlev, "Development stages, structure, and turbulent characteristics of compressible separated flows in the vicinity of two-dimensional obstacles," Preprint No. 27-86, Inst. Theor. and Appl. Mech., Sib. Div., Acad. of Sci. of the USSR, Novosibirsk (1986).
15. A. A. Zheltovodov, V. M. Trofimov, É. Kh. Shilein, and V. N. Yakovlev, "Documented data of experimental studies of supersonic turbulent separated flows in the vicinity of oblique steps and ledges," Report No. 2030, Inst. Theor. and Appl. Mech., Sib. Div., Acad. of Sci of the USSR, Novosibirsk (1990).
16. A. A. Zheltovodov and C. C. Hortsman, "Experimental and numerical investigation of 2-D expansion/shock wave-turbulent boundary layer interactions," Preprint No. 2-93, Inst. Theor. and Appl. Mech., Sib. Div., Russian Acad. of Sci., Novosibirsk (1993).
17. C. C. Hortsman and A. A. Zheltovodov, "Numerical simulation of shock waves/expansion fans-turbulent boundary layer interaction," in: Proc. Int. Conf. on the Methods of Aerophysical Research, August 22–26, 1994, Novosibirsk (1994), Part 2, pp. 118–125.
18. I. A. Graur, T. G. Elizarova, and B. N. Chetvertushkin, "Modeling of complicated gas-dynamic flows on the basis of kinetic algorithms," *Differ. Uravn.*, **22**, No. 7, 1173–1180 (1986).
19. I. A. Graur, T. G. Elizarova, and B. N. Chetvertushkin, "Numerical modeling of turbulent flow past an oblique step," *Mat. Model.*, **3**, No. 11, 31–44 (1990).
20. A. V. Borisov, A. A. Zheltovodov, D. Badekas, and N. Narayanswami, "Numerical investigation of supersonic turbulent flows in the vicinity of oblique steps," *Prikl. Mekh. Tekh. Fiz.*, **36**, No. 2, 68–80 (1995).
21. A. V. Borisov and V. B. Karamyshev, "A method for numerical investigation of turbulent separated flows," Preprint No. 9-88, Inst. Theor. and Appl. Mech., Sib. Div., Acad. of Sci. of the USSR, Novosibirsk (1988).
22. A. V. Borisov and V. B. Karamyshev, "Numerical simulation of separated turbulent flows," *Izv. Sib. Otdel. Akad. Nauk SSSR, Ser. Tekh. Nauk*, No. 1, 37–43 (1990).
23. A. V. Borisov, N. N. Fedorova, and S. I. Shpak, "Numerical simulation of a turbulent separation based on the averaged Navier–Stokes equations," Proc. Int. Conf. on the Methods of Aerophysical Research, August 22–26, 1994, Novosibirsk (1994), Part 2, pp. 55–61.

24. A. I. Maksimov, A. A. Pavlov, and A. M. Shevchenko, "Development of the skin friction measurement technique for supersonic gradient flows," *ibid.*, pp. 172–176.
25. A. V. Borisov, S. S. Vorontsov, A. A. Zheltovodov, et al., "Development of experimental and computational methods for supersonic turbulent flows," Preprint No. 9-93, Inst. Theor. and Appl. Mech., Sib. Div., Russian Acad. of Sci., Novosibirsk (1993).
26. W. K. Anderson, J. L. Thomas, Bram van Leer, "Comparison of finite volume flux vector splitting for the Euler equations," *AIAA J.*, **24**, No. 9, 1453–1460 (1986).
27. P. Woodward and P. Colella, "The numerical simulation of two-dimensional fluid flow with strong shocks," *J. Comput. Phys.*, **54**, No. 1, 115–173, (1984).
28. B. Edney, "Anomalous heat transfer and pressure distributions on blunt bodies at hypersonic speeds in the presence of an impinging shock," Report No. 115, Aeron, Res. Inst. of Sweden (1968).